

## Electron paramagnetic resonance and photo-electron paramagnetic resonance investigation on the recharging of the substitutional nitrogen acceptor in ZnO

J. E. Stehr, D. M. Hofmann, and B. K. Meyer

Citation: *J. Appl. Phys.* **112**, 103511 (2012); doi: 10.1063/1.4765729

View online: <http://dx.doi.org/10.1063/1.4765729>

View Table of Contents: <http://jap.aip.org/resource/1/JAPIAU/v112/i10>

Published by the American Institute of Physics.

---

### Additional information on J. Appl. Phys.

Journal Homepage: <http://jap.aip.org/>

Journal Information: [http://jap.aip.org/about/about\\_the\\_journal](http://jap.aip.org/about/about_the_journal)

Top downloads: [http://jap.aip.org/features/most\\_downloaded](http://jap.aip.org/features/most_downloaded)

Information for Authors: <http://jap.aip.org/authors>

## ADVERTISEMENT

The advertisement banner for AIP Advances features a green and yellow background with abstract wavy lines. The text 'AIPAdvances' is prominently displayed in the center, with 'AIP' in blue and 'Advances' in green. To the right, a circular seal states 'Now Indexed in Thomson Reuters Databases'. Below the main title, a blue bar contains the text 'Explore AIP's open access journal:', followed by a list of three bullet points: 'Rapid publication', 'Article-level metrics', and 'Post-publication rating and commenting'.

**AIPAdvances**

Now Indexed in  
Thomson Reuters  
Databases

**Explore AIP's open access journal:**

- Rapid publication
- Article-level metrics
- Post-publication rating and commenting

# Electron paramagnetic resonance and photo-electron paramagnetic resonance investigation on the recharging of the substitutional nitrogen acceptor in ZnO

J. E. Stehr,<sup>1,2,a)</sup> D. M. Hofmann,<sup>1</sup> and B. K. Meyer<sup>1</sup>

<sup>1</sup>Physikalisches Institut, Justus-Liebig-University Giessen, Heinrich-Buff-Ring 16, 35392 Giessen, Germany

<sup>2</sup>Department of Physics, Chemistry, and Biology, Linköping University, 581 83 Linköping, Sweden

(Received 2 October 2012; accepted 17 October 2012; published online 21 November 2012)

We investigated the substitutional nitrogen center in ZnO single crystals by electron paramagnetic resonance (EPR) and photo-EPR spectroscopy. Aside the three principle hyperfine lines due to the interaction of the  $N^0$  (2p5) electron spin with the nitrogen nucleus ( $I=1$ , natural abundance 99.6%), we identify additional satellite lines which arise from  $\Delta m_S = \pm 1$  and  $\Delta m_I = \pm 1, \pm 2$  transitions becoming allowed due to quadrupole interaction. The quadrupole coupling constant  $e^2qQ/h$  is determined to  $-5.9$  MHz with an asymmetry parameter of  $\eta=0.05$ . These values are somewhat different from those obtained for the nitrogen center in ZnO powders, but are closer to the theoretical calculations of Gallino *et al.* We further carefully investigated the photon induced recharging of the N centers. We determine the energy  $h\nu$  required for the process  $N_O^- + h\nu \rightarrow N_O^0 + e_{cb}^-$  to  $2.1 \pm 0.05$  eV, the dependence of the EPR signal intensity on the illumination time shows a mono-exponential behavior which gives evidence that a direct ionization process is monitored. © 2012 American Institute of Physics. [<http://dx.doi.org/10.1063/1.4765729>]

## I. INTRODUCTION

A straight forward approach to incorporate acceptors into ZnO could be to test the doping of the group V elements of the periodic table. The group V elements might substitute an oxygen lattice-site and thus act as acceptors. Considering the ionic radii, nitrogen comes closest to oxygen and thus seems to be the most promising candidate. Indeed isolated nitrogen acceptors ( $N_O$ ) were identified by electron paramagnetic resonance (EPR) spectroscopy.<sup>1–3</sup> The EPR signals of the isolated nitrogen centers were first observed in nominally undoped ZnO single crystals and later also in ammonia treated ZnO powders.<sup>4,5</sup> To our knowledge, the isolated nitrogen acceptors were never observed in intentionally doped epitaxial films or single crystals, although evidence for the presence of high concentrations of nitrogen was obtained by other characterization methods.<sup>6–8</sup>

For the EPR experiments on the N centers the samples had to be illuminated by light to convert them to the paramagnetic charge state ( $N^0$ ).<sup>1–3</sup> This illumination was needed because residual shallow donors were present in the samples causing the nitrogen centers to be in the negative EPR inactive charge state ( $N^-$ ). It was noticed that photon energies of about 2.4 eV were already sufficient to carry out this conversion process and in comparison to the band gap energy of 3.4 eV it might give already a hint that isolated nitrogen is a deep level center, rather than being a shallow acceptor. A level position of approximately 1 eV above the valence band would rule out nitrogen making an efficient p-type dopant.

However, the recharging of the nitrogen center might be induced by indirect processes caused by other intrinsic or

extrinsic defects in the samples. For example, it is quite common to observe sub-band gap absorption in ZnO starting at energies of about 2 eV, this is related to the yellowish appearance of some crystals. The microscopic origin is not always clear, plasmon-absorption due to Zn-nano-droplets are discussed as well as the absorption due to intrinsic centers or impurities.<sup>9</sup>

This situation was our motivation to examine the recharging behavior of the substitutional nitrogen in ZnO in more detail by photo-EPR investigations in the spectral range from 0.7 eV up to 3.4 eV. We determine the energy  $h\nu$  required for the process  $N_O^- + h\nu \rightarrow N_O^0 + e_{cb}^-$  to  $2.1 \pm 0.05$  eV. The dependence of the EPR signal intensity on the illumination time shows a mono-exponential behavior which gives evidence that a direct process is monitored. These results give strong evidence that the isolated nitrogen acceptors are deep level defects and cannot be responsible for the occasionally observed p-type conductivity of some ZnO samples. Similar conclusions were recently drawn from optical experiments and theoretical calculations.<sup>5,10,11</sup>

## II. EXPERIMENTAL DETAILS

For our experiments, we used pieces of standard commercial ZnO wafers supplied by Eagle Picher Co. (Miami). The crystals were grown by the seeded chemical vapor transport and had a slight yellow coloration. They were n-type conducting with a carrier concentration of about  $8 \times 10^{17} \text{ cm}^{-3}$ . The samples were irradiated with 3.8 MeV electrons with a dose of  $2 \times 10^{18} \text{ cm}^{-2}$ . Such procedure is known to reduce the carrier concentration,<sup>2,3</sup> in our case to  $n \sim 5 \times 10^{14} \text{ cm}^{-3}$  as determined by Hall measurements at room temperature. The total concentration of nitrogen in the crystals was obtained from secondary ion mass

<sup>a)</sup>Electronic mail: [janst@ifm.liu.se](mailto:janst@ifm.liu.se).

spectroscopy to  $N = (4 \pm 2) \times 10^{18} \text{ cm}^{-3}$ . Thus the total concentration of nitrogen is much higher than the concentration of substitutional nitrogen centers observable by EPR ( $\sim 5 \times 10^{16} \text{ cm}^{-3}$ ). The EPR measurements were carried out with a Bruker ESP 900 spectrometer operating at 9 GHz equipped with an Oxford He-flow cryostat and a microwave resonator allowing optical access to the sample. For the illumination, a high pressure mercury lamp was used and the wavelength selection was done by inserting appropriate band pass filters with a half width of less than 25 nm in the optical path. Also neutral density filters were used to provide the same light intensity for the complete wavelength range. All EPR measurements were done at a temperature of about 5 K and at low microwave powers to avoid saturation effects of the signal.

### III. EPR ANALYSIS

To analyze the EPR spectra, the following Spin-Hamilton operator:

$$\mathcal{H} = \mu B g S + S A I + I Q I - g_N \mu_N B I \quad (1)$$

was used.<sup>5</sup> The first term denotes the Zeeman energy of the electron spin  $S$  in the static magnetic field  $B$ ; the second term describes the hyperfine interaction  $A$  with the nitrogen nucleus ( $I = 1$ , 99.6% natural abundance); the third term accounts for a quadrupole interaction  $Q$  arising for nuclei with spin  $I \geq 1/2$  from the interaction with an electric field gradient at the site of the nucleus, the last term gives the nuclear Zeeman energy. For the nitrogen center considered here, the electron  $g$ -tensor reduces to two  $g$ -values, parallel ( $g_{\parallel}$ ) and perpendicular ( $g_{\perp}$ ) to the crystallographic  $c$ -axis of the ZnO crystal. We also give the hyperfine interaction constants ( $A_{\parallel}$ ,  $A_{\perp}$ ) with respect to this axis to allow for an easy comparison to the published data.<sup>1,2,5</sup>  $A_{\parallel}$  and  $A_{\perp}$  can be expressed in terms of an isotropic part  $a$  (Fermi-contact interaction) and an anisotropic part  $b$ , by  $A_{\parallel} = a + 2b$ , and  $A_{\perp} = a - b$ .

The nuclear quadrupole tensor  $\mathbf{Q}$  is related to the quadrupole coupling constant  $K = e^2 q Q / (4I(2I-1))$  by  $Q_x = -K(1 - \eta)$ ,  $Q_y = -K(1 + \eta)$ , and  $Q_z = 2K$ , with  $\eta$  the asymmetry parameter. All other symbols in Eq. (1) have their usual meaning.

A typical EPR spectrum of the N-center is shown in Fig. 1. The three principle lines labeled N1 to N3 are due to the hyperfine splitting with the central nitrogen nucleus nuclear spin  $I = 1$  with an abundance of 99.6%. These signals represent the allowed EPR transitions which obey the usual selection rules  $\Delta m_S = \pm 1$  and  $\Delta m_I = 0$ . The magnetic field positions of these signals change upon rotation of the sample with respect to the static magnetic field  $B$  (Fig. 2). From the angular dependence, we analyze the hyperfine interaction and the  $g$ -values and obtain  $g_{\perp} = 1.963$  and  $g_{\parallel} = 1.995$ , and  $A_{\perp} = 8.5 \text{ MHz}$  and  $A_{\parallel} = 81.1 \text{ MHz}$ . These values are within the experimental accuracy in very good agreement to previous studies and theoretical calculations,<sup>1,2,5</sup> thus there is no doubt that all research groups investigate the same defect. The full analysis of the Spin-Hamiltonian parameters in the

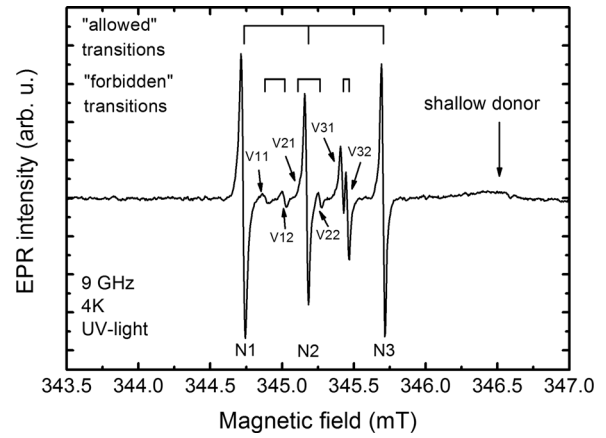


FIG. 1. 9 GHz EPR spectrum of the substitutional nitrogen centers in ZnO. The allowed hyperfine transitions due to the interaction with the N nucleus ( $I = 1$ , 99.6% natural abundance) are labeled N1, N2, and N3. The weaker transitions V11 to V32 become observable due to additional nuclear quadrupole interaction.

wurtzite symmetry of ZnO requires measuring the EPR resonance signals in the plane perpendicular to the crystal  $c$ -axis. In this orientation, we find an isotropic signal with  $g = 1.966$  and a hyperfine coupling constant of  $A = 10.2 \text{ MHz}$ . The Spin-Hamilton parameters were obtained by fitting the angular dependent EPR data with Eq. (1) using Easy-Spin.<sup>12</sup>

For the three intense hyperfine lines (N1 to N3), one would expect that they are of equal height, which is clearly not the case in the spectrum of Fig. 1. The reason is that this spectrum was taken at a rather high microwave power which induces saturation effects. In the following, we investigated the tiny resonances in between N1 to N3 in more detail. We label these six lines with “v” (verboten: forbidden), to indicate that these resonances appear due to  $\Delta m_S = \pm 1$  and  $\Delta m_I = \pm 1, \pm 2$  transitions, thus violating the “usual” selection rules. A scheme to illustrate the appearance of these lines is given in Fig. 3. It also shows that the appearance of the v-resonances allows determining the parameters of the quadrupole interaction term (the lines were also observed in the measurements with the crystal plane perpendicular to the

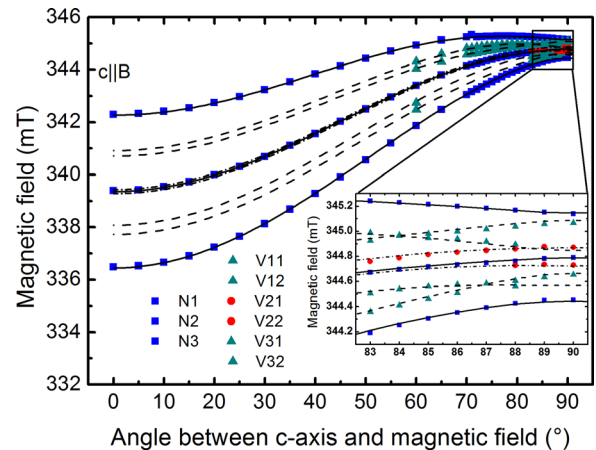


FIG. 2. EPR resonance positions of the substitutional nitrogen center in ZnO for rotating the crystal  $c$ -axis from orientations  $\parallel$  to  $\perp$  in respect to the external static magnetic field. The drawn lines represent simulations with the best fitting parameters.

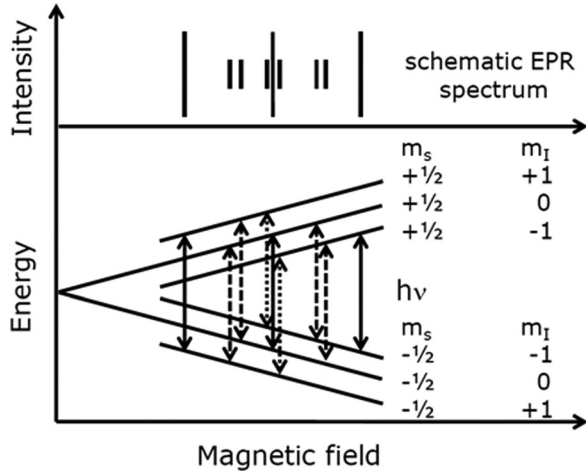


FIG. 3. Scheme to illustrate the appearance of the resonances labeled V in Figure 1, they arise from  $\Delta m_s = \pm 1$  and  $\Delta m_I = \pm 1$  (dashed arrows),  $\pm 2$  (dotted arrows) transitions becoming allowed due to quadrupole interaction.

c-axis). We obtain for the quadrupole coupling constant  $e^2qQ/h = -5.9$  MHz and the asymmetry parameter  $\eta = 0.05$ .

These values are comparable to  $|e^2qQ/h| = 5.3$  MHz and  $\eta = 0.2$  reported for the nitrogen centers in ZnO powder and 6.1 MHz and  $\eta = 0.00$  obtained from the density functional calculation presented in the same paper.<sup>5</sup> Especially, the asymmetry parameter  $\eta$  determined from our experiments is closer to the one predicted by the calculations. It may indicate that the granular structure of the powders introduces additional electrical field components at the position of the N-nucleus, and/or that  $N_O^0$  in the ZnO powders is located in surface near positions. However, as mentioned in Ref. 5 the investigations yield that the spin density of  $N^0$  in ZnO is located by more than 95% in a p-type orbital.

#### IV. PHOTO-EPR

From the technological as well as scientific point of view, it is very important to decide whether nitrogen forms a shallow or a deep acceptor in ZnO. Therefore, we investigated the wavelength dependent creation process of the nitrogen EPR signal. For each measurement at a given specific wavelength, the sample was cooled down from room temperature to 4 K in dark to have the same initial condition for each measurement in order to avoid effects of ambient light and photon induced recharging from previous measurements. Furthermore, the EPR signal intensities obtained by those measurements have to be corrected due to the fact that the optical absorption of the sample is also wavelength dependent, as described by Godlewski.<sup>13</sup> Since the EPR intensity is proportional to the square root of the light intensity, the correction factor  $\sqrt{1 - \exp(-\alpha d)}$  is introduced. The values of  $\alpha d$  were obtained by optical transmittance and reflectance measurements on our samples. Figure 4 shows the spectral dependence of the EPR intensity of the paramagnetic nitrogen center. One can see that the threshold energy to convert the nitrogen center into its paramagnetic charge state is 1.95 eV. In order to determine the ionization cross section, the data were analyzed by the following equations:<sup>13</sup>

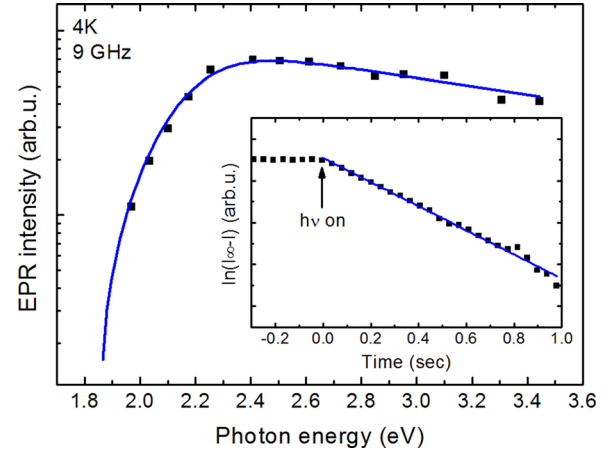


FIG. 4. Intensity of the EPR spectrum of the  $N_O$  center upon illumination of the sample with photon energies between 1.8 eV and 3.5 eV (full squares). The drawn line was calculated according to Eqs. (2) and (3). Inset: Time dependence of the  $N_O$  acceptor EPR signal intensity after switching on the light source. The linear slope indicates a mono-exponential process, i.e., a direct recharging process.

$$\sigma_{el}(E_{opt}, h\nu) \sim \frac{\sqrt{h\nu - E_{opt}}}{(h\nu)^3}, \quad (2)$$

here  $\sigma_{el}$  denotes the optical cross section,  $h\nu$  the photon energy, and  $E_{opt}$  the optical ionization energy. Taking electron phonon-interaction into account one obtains

$$\sigma_0(h\nu) = \frac{1}{\sqrt{\pi}} \int_{-\beta}^{\infty} e^{-z^2} \sigma_{el}(E_{opt}, h\nu + \Gamma) \left(1 + \frac{\Gamma}{h\nu}\right) dz \quad (3)$$

with

$$\beta = \frac{h\nu - E_{opt}}{\Gamma}, \quad (4)$$

where  $\Gamma$  describes the broadening of the photo transition absorption band at elevated temperatures

$$\Gamma = \frac{\omega_0}{\omega_{ex}} \sqrt{2(E_{opt} - E_{th})\hbar\omega_0 c \hbar \left(\frac{\hbar\omega_0}{2k_B T}\right)}. \quad (5)$$

The dependence of the experimental data on the photon energy (Fig. 4) is well reproduced by the parameters  $E_{opt} = 2.1 \pm 0.05$  eV and  $\Gamma = 0.26 \pm 0.05$  eV (full line in Fig. 4).

Further information on the recharging behavior of the defect can be obtained by its time dependency. In these experiments, the magnetic field position is held at a constant value and the EPR signal intensity is monitored as a function of the time. Such measurement is shown in the inset of Figure 4. The time at which the UV light was switched on is marked by the arrow. One can clearly see the linear behavior of the slope, what corresponds to a mono-exponential behavior, since the data are plotted on a logarithmic scale. Such a mono-exponential behavior indicates a direct charging process of the nitrogen center from its non-paramagnetic state into the paramagnetic one.

In a next step, we tried to measure the optical transition to the valence band. To achieve this, an EPR experiment at



4 K was performed in which the sample was illuminated first with 325 nm light of a high pressure mercury lamp with a band pass filter to create the paramagnetic nitrogen center. Simultaneously light with wavelengths ranging from 980 nm to 660 nm of various laser diodes was coupled into the sample to lift an electron from the valence band to the defect, which should quench the EPR signal. Unfortunately, it was not possible to observe such quenching of the EPR signal. A possible explanation for such behavior would be a considerable smaller cross-section for this process compared to the electron transfer to the conduction band.

Recently, Tarun *et al.*<sup>11</sup> performed a comprehensive study on ZnO crystals containing nitrogen-hydrogen complexes which were monitored by infrared absorption line at  $3148\text{ cm}^{-1}$  (Refs. 11 and 14). Upon annealing at temperatures above  $775^\circ\text{C}$ , these centers dissociated into their fragments and a broad photoluminescence band at 1.7 eV (energy of its intensity maximum at room temperature) showed up in line with this process. For the onset of excitation of the 1.7 eV emission band, an energy of 2.2 eV was determined. It corresponds to the onset of the  $\text{N}_\text{O}^- + h\nu \rightarrow \text{N}_\text{O}^0 + \text{e}_{\text{cb}}^-$  process for which we determined here  $2.1 \pm 0.05\text{ eV}$  from the photo-EPR experiments.

In addition, also first-principle computations using hybrid functionals performed by Lyons, Janotti, and Van de Walle support the deep level character of the nitrogen center.<sup>15</sup> Their calculations show that the  $\text{N}_\text{O}$  is a deep acceptor with the (0/-) level 1.3 eV above valence band maximum. Optical absorption and emission energies of 2.4 and 1.7 eV, respectively, were estimated from a configuration-coordinate diagram analysis. The total Frank-Condon shift (absorption and emission) of 0.7 eV is due to large lattice relaxation. The experimental values for the onset of the absorption process determined here and in Ref. 11 are somewhat smaller ( $\sim 2.1\text{--}2.2\text{ eV}$ ) and adopting the relaxation energy given in Ref. 15 of around 0.3 eV, we estimate the level position at  $E_{\text{vb}} + 1.6\text{ eV}$ .

## V. SUMMARY

In summary, our EPR and photo-EPR experiments clearly show that the  $\text{N}_\text{O}$  defect in ZnO is a deep acceptor and therefore can hardly account for the p-type conductivity occasionally observed in the material. The results are in accordance to the results obtained earlier from experiments using optical spectroscopy and theoretical considerations. Thus the p-type conductivity of nitrogen doped ZnO is likely to be caused by more complex species. Nitrogen pair formation was recently considered,<sup>16</sup> but demands experimental verification by structure sensitive methods.

<sup>1</sup>W. E. Carlos, E. R. Glaser, and D. C. Look, *Physica B* **308–310**, 976 (2001).

<sup>2</sup>N. Y. Garces, N. C. Giles, L. E. Halliburton, G. Cantwell, D. B. Eason, D. C. Reynolds, and D. C. Look, *Appl. Phys. Lett.* **80**, 1334 (2002).

<sup>3</sup>N. Y. Garces, L. J. Wang, N. C. Giles, L. E. Halliburton, G. Cantwell, and D. B. Eason, *J. Appl. Phys.* **94**, 519 (2003).

<sup>4</sup>D. Pfisterer, J. Sann, D. M. Hofmann, M. Plana, A. Neumann, M. Lerch, and B. K. Meyer, *Phys. Status Solidi B* **243**, R1 (2006).

<sup>5</sup>F. Gallino, C. Di Valentin, G. Pacchioni, M. Chiesa, and E. Giamello, *J. Mater. Chem.* **20**, 689 (2010).

<sup>6</sup>F. Reuss, C. Kirchner, T. Gruber, R. Kling, S. Maschek, W. Limmer, A. Waag, and P. Ziemann, *J. Appl. Phys.* **95**, 3385 (2004).

<sup>7</sup>B. K. Meyer, J. Sann, D. M. Hofmann, C. Neumann, and A. Zeuner, *Semicond. Sci. Technol.* **20**, S62 (2005).

<sup>8</sup>A. Zeuner, H. Alves, D. M. Hofmann, B. K. Meyer, A. Hoffmann, U. Haboeck, M. Strassburg, and M. Dworzak, *Phys. Status Solidi B* **234**, R7 (2002).

<sup>9</sup>K. Irscher, M. Albrecht, B. Heimbrodt, M. Naumann, T. Remmele, D. Schulz, T. Schulz, and R. Fornari, *Phys. Status Solidi C* **6**, 2658 (2009).

<sup>10</sup>A. Janotti and C. G. Van de Walle, *Phys. Rev. B* **76**, 165202 (2007).

<sup>11</sup>M. C. Tarun, M. Z. Iqbal, and M. D. McCluskey, *AIP Adv.* **1**, 022105 (2011).

<sup>12</sup>S. Stoll and A. Schweiger, *J. Magn. Reson.* **178**, 42 (2006).

<sup>13</sup>M. Godlewski, *Phys. Status Solidi A* **90**, 11 (1985).

<sup>14</sup>S. J. Jokela, M. C. Tarun, and M. D. McCluskey, *Physica B* **404**, 4810 (2009).

<sup>15</sup>J. L. Lyons, A. Janotti, and C. G. V. d. Walle, *Appl. Phys. Lett.* **95**, 252105 (2009).

<sup>16</sup>S. Lautenschlaeger, M. Hofmann, S. Eisermann, G. Haas, M. Pinnisch, A. Laufer, and B. K. Meyer, *Phys. Status Solidi B* **248**, 1217 (2011).